Acquisition of plasmids conferring carbapenem and aminoglycoside resistance and loss of surface-exposed macromolecule structures as strategies for the adaptation of *Acinetobacter baumannii* CC104^O/CC15^P strains to the clinical setting

María M. Cameranesi[1]†, Julian Paganini[1]†, Adriana S. Limansky[1], Jorgelina Moran-Barrio[1], Suzana P. Salcedo[2], Alejandro M. Viale[1],* and Guillermo D. Repizo[1,2],*

Abstract

Acinetobacter baumannii (*Aba*) is an emerging opportunistic pathogen associated to nosocomial infections. The rapid increase in multidrug resistance (MDR) among *Aba* strains underscores the urgency of understanding how this pathogen evolves in the clinical environment. We conducted here a whole-genome sequence comparative analysis of three phylogenetically and epidemiologically related MDR *Aba* strains from Argentinean hospitals, assigned to the CC104^O/CC15^P clonal complex. While the Ab244 strain was carbapenem-susceptible, Ab242 and Ab825, isolated after the introduction of carbapenem therapy, displayed resistance to these last resource *β*-lactams. We found a high chromosomal synteny among the three strains, but significant differences at their accessory genomes. Most importantly, carbapenem resistance in Ab242 and Ab825 was attributed to the acquisition of a Rep_3 family plasmid carrying a bla_{OXA-58} gene. Other differences involved a genomic island carrying resistance to toxic compounds and a Tn*10* element exclusive to Ab244 and Ab825, respectively. Also remarkably, 44 insertion sequences (ISs) were uncovered in Ab825, in contrast with the 14 and 11 detected in Ab242 and Ab244, respectively. Moreover, Ab825 showed a higher killing capacity as compared to the other two strains in the *Galleria mellonella* infection model. A search for virulence and persistence determinants indicated the loss or IS-mediated interruption of genes encoding many surface-exposed macromolecules in Ab825, suggesting that these events are responsible for its higher relative virulence. The comparative genomic analyses of the CC104^O/CC15^P strains conducted here revealed the contribution of acquired mobile genetic elements such as ISs and plasmids to the adaptation of *A. baumannii* to the clinical setting.

DATA SUMMARY

The authors confirm all supporting data, code and protocols have been provided within the article or through the Supplementary Material (available in the online version of this article).

INTRODUCTION

Acinetobacter baumannii (*Aba*) nowadays represents an important cause of infections in healthcare institutions worldwide generally affecting immunocompromised and severely injured patients [1–3]. Infections due to *Aba*, rarely reported before the 1970s, have dramatically increased during the last three decades paralleling the global spread of a limited number of epidemic clonal complexes (CC) displaying multidrug resistant (MDR)-phenotypes, and from which CC2 and CC1 are the best characterized lineages, and conforming thus the international clone (IC) II and I, respectively [2, 4]. A most worrisome problem in the actuality is the rapidly increasing resistance to last-resort carbapenems among *Aba* strains of the different CC [1–3, 5]. *Aba* carbapenem resistance arises from different factors that

encompass as the main cause the acquisition of carbapenemase genes belonging to different carbapenem-hydrolysing class D β-lactamases (CHDL) classes including bla_{OXA-23}, bla_{OXA-58} and $bla_{OXA24/40}$, added to reductions of permeability due to the mutation of specific outer-membrane (OM) channels and efflux pumps [5–10]. The analysis of the origin and dissemination of antimicrobial resistance (AR) genes among MDR pathogens constitutes a research priority [11]. In this context, the molecular basis of resistance acquisition among *Aba* strains, and in particular among the less studied CCs, remains poorly resolved.

It is generally thought that *Aba* pathogenicity results from the combination of a remarkable ability to survive unfavourable environmental conditions, added to a high genomic plasticity and ability to acquire genes by horizontal gene transfer (HGT) [3, 12–14]. Most *Aba* clinical strains invariably contain many acquired mobile genetic elements (MGE) of strong adaptive significance, including different plasmids and chromosomally located resistance islands (RI), encompassing several transposons and integrons, which play pivotal roles in both antimicrobial and heavy-metal ion resistances [2, 12, 15–18]. Furthermore, other traits that might be beneficial for survival in the host are carried by MGEs, including virulence factors, detoxifying mechanisms and genes for secondary metabolism pathways [2]. In addition, these strains carry a large repertoire of insertion sequences (ISs) capable not only of mediating gene disruptions but also large genome rearrangements, thus providing bacterial cells with an outstanding ability to rapidly respond to new environmental challenges contributing to a rapid adaptation to the clinical environment [19, 20].

AR derived from gene acquisition and/or mutation is generally considered a main determinant of the success of particular *Aba* strains in the nosocomial environment [2, 3, 5]. In contrast, virulence traits and the pathogenic potential of certain *Aba* lineages are less well defined [3, 5, 21]. As in other pathogens, a number of macromolecular structures have been associated to virulence including a capsular polysaccharide that protects cells from host complement killing and phagocytosis, a biofilm related to adhesion and motility, OM proteins (OMP) such as OmpA involved in host-cell recognition, internalization and pathogenicity, a lipooligosaccharide influencing host innate immune responses, iron capture systems, phospholipases C and D [3, 5, 22]. Notably, most genes related to the above functions are encoded in the core genome of the *Aba* clinical strains analysed, regardless of their affiliation to particular CCs or to sporadic isolates [2]. It thus remains an open question whether pathogenicity may arise by a differential regulation of virulence genes depending on the CC lineage (or even on internal lineages inside a given CC), on the polymorphic differences in shared virulence genes, or a combinatorial effect of multiple genes [2].

Whole-genome-sequence (WGS) comparisons have become a common place in examining strain-to-strain variability and in comparing pathogenic strains with environmental isolates, allowing the identification of underlying genetic determinants and mechanisms responsible for the observed phenotypic dissimilarities [23, 24]. When applied to *Aba*, WGS approaches have shed light on the mechanisms of acquisition and evolution

Impact Statement

Acinetobacter baumannii is an ESKAPE opportunistic pathogen cause of healthcare-associated infections worldwide. The majority of infections are caused by strains belonging to a limited number of globally spread clonal complexes (CC), exhibiting multidrug resistance (MDR) including to the last-resort carbapenems. MDR, is a main determinant of *A. baumannii* success in the nosocomial environment, and the molecular basis of its dissemination represents a research priority. Also, the *A. baumannii* traits enabling infection and persistence in the clinical setting are poorly resolved, particularly among the less-studied CC. Here, we conducted whole-genome sequence comparative analysis of three phylogenetically and epidemiologically related MDR *A. baumannii* strains of the CC104[O]/CC15[P] prevalent in South America, displaying different carbapenem-resistance phenotypes. We aimed to uncover the genetic events involved in their adaptation to the local clinical environment. This analysis revealed that different mobile genetic elements such as resistance plasmids and insertion sequences cooperatively contribute to genomic remodelling, thus securing adaptation and subsequent persistence of infective strains. A deep understanding of the strategies used by this pathogen to escape from antimicrobial treatment and host defenses is crucial for the adoption of measures aimed to limit its further dissemination.

of AR, population dynamics and epidemiology [2, 5, 23]. WGS have also illustrated extensive and redundant AR gene carriage and provided direct evidence of HGT and homologous recombination between *Aba* strains since their entry into the hospital, facilitating the adaptation of particular lineages to the prevailing clinical conditions [25, 26]. We have previously characterized the OMP variability among three genotypically closely related MDR *Aba* strains displaying different β-lactam susceptibility phenotypes, Ab242, Ab244 and Ab825, which were isolated from patients hospitalized in the Hospital de Emergencias Clemente Alvarez (HECA) of Rosario, Argentina [7, 8, 27, 28]. Ab244, originally characterized as ST39 [8] and re-designated ST104 following the MLST Oxford scheme [21], represents a sporadic strain isolated in 1997. This strain showed resistance to β-lactams such as ceftazidime, which constituted the antibiotic therapy employed for infections associated by MDR *Aba* at the hospital at this period. Ab242 is the representative strain of a carbapenem-resistant (Carb^R) outbreak that occurred in the same year, and which followed the introduction of imipenem (IPM) therapy for the treatment of MDR bacterial infections [27]. The isolates of this clone showed either intermediate (16 µg ml^{-1}) or resistant ($\geq$32 µg ml^{-1}) MIC values to ceftazidime [29]. Finally, Ab825 is a sporadic strain showing both ceftazidime and carbapenem resistance, and was isolated a year after the outbreak was controlled [27]. Our previous studies [8, 28] indicated substantial allelic variability at the level of the *carO*

Table 1. General traits and genomic features of *A. baumannii* strains under study

	Strains		
	Ab242	**Ab244**	**Ab825**
General traits*1			
Former designation/alias	24214	24474	825
Isolation date	1997-10-01	1997-10-01	1999-03-01
Specimen/source	ascitic fluid	blood	wound
Carbapenem susceptibility Phenotype	Resistant	Susceptible	Resistant
Genomic parameters*2			
Depth of coverage	47.6x	25.9x	103.0x
Number of contigs	107	99	99
Estimated size (Mbp)	4	3.9	3.9
GC content (%)	39.2	39.1	39.1
Number of CDSs	3722	3659	3614
Number of tRNA genes	61	64	63
Number of rRNA operons	3	3	3
Prophage regions	4	3	4
ISs	12	10	45
Complete plasmids	3 (accession numbers KY984045.1, KY984046.1 And KY984047.1)	1 (accession number MG520098)	2 (accession numbers MG100202.1 And MG100203.1
BioProject	PRJNA398382	PRJNA398382	PRJNA398382
Biosample	SAMN07509424	SAMN08028494	SAMN07573381
Accession	NXGW00000000	PGTR00000000	NTFR00000000

*1 See reference 27.
*2 Based on NCBI Prokaryotic annotation pipeline.

gene, encoding the second most abundant OMP of the *Aba* OM involved in IPM uptake. Ab244 and Ab242 harbour different *carO* alleles, namely *carO* variant II and *carO* variant III alleles, respectively [8]. In contrast, Ab825 carries a disrupted *carO* variant III gene due to the natural insertion (and selection) of an IS*Aba825* element [6].

In this work we performed a WGS comparative characterization of these three MDR *Aba* strains to evaluate in more detail their genetic variability and underlying causes, in an attempt to understand the mechanisms of adaptation and persistence of these genetically and epidemiologically closely related strains in the hospital environment.

METHODS

A. baumannii strains

Ab244, Ab242 and Ab825 (Table 1) are epidemiologically related MDR *Aba* strains from clinical specimens obtained from in-patients of the HECA. These three strains formed a clonal group as judged by a combination of genotypic procedures including OD-PCR, repetitive extragenic palindromic-PCR (REP-PCR), and PFGE [27].

Genomic sequencing, assembly and annotation

Ab242 and Ab244 genomic DNA was isolated using a commercial kit (Wizard Genomic DNA purification kit, Promega), following the manufacturer's protocols. The corresponding genomic sequences were obtained using a paired-end strategy with a 454 pyrosequencer (Life Science Corporation) at the Instituto de Agrobiotecnología Rosario (INDEAR, Argentina). Quality-filtered reads were *de novo* assembled using Newbler v2.5.3. Ab825 genomic DNA was isolated using the DNeasy Blood and Tissue kit (Qiagen) following the manufacturer's protocols. The genomic sequence was obtained in this case using a paired-end strategy using an Illumina MiSeq sequencer at the National Institute of Health (Lisbon, Portugal). Reads were subjected to quality assessment and further assembled using Velvet version 1.2.10. The *de novo* assembly process was optimized using the Velvet Optimiser script version 2.2.5.

For each genome, the resulting contigs were ordered and oriented with Mauve [30] using the *Aba* ATCC17978 genome as a reference (CP012004). The replication origins (*oriC*) were predicted by OriFinder [31]. All three assembled genome

sequences were annotated using the NCBI Prokaryotic annotation pipeline.

Presence of mobile genetic elements in the genomes was investigated by the following online tools and/or open-access database and manual examinations: IS Finder [32] for insertion sequence (IS) elements. IS insertion sites were inferred from draft genome assemblies by identifying fragments of the inverted repeats corresponding to these mobile elements at contig edges. Putative prophage sequences were identified by PHASTER analysis [33]. Genes encoding AR were identified with ResFinder 2.1 [34]. Assignments of sequence types (STs) for the three strains under study were done using the sequences of the housekeeping genes employed by each scheme [35].

In order to evaluate the occurrence and distribution of the various iron uptake systems reported for *Aba*, we first downloaded the complete genomes of 132 publicly available strains. We then performed BLASTN searches using as query the nucleotide sequences of the iron uptake clusters from *Aba* ACICU strain [36], with a minimal coverage length and sequence identity of 80 and 90%, respectively. An identical approach was followed when analysing the presence of the *cpaA* gene, but in this case we used the nucleotide sequence of strain AB031 as query.

A. baumannii Ab244 plasmid assembly and analysis

A contig-encoding plasmid sequences was assembled from the pyrosequencing data derived from Ab244 strain. The circular structure of this plasmid was then verified by gap closure of contigs using PCR with specifically designed primer pairs (Table S1, Fig. S3, available in the online version of this article). All amplicons were subjected to sequence verification at the Sequencing Facility of Maine University.

Galleria mellonella infection assays

G. mellonella larvae were purchased from Sud Est Appats (http://www.sudestappats.fr/) and were used the day after arrival. Groups of 20 randomly picked larvae were used for each assay condition. Infections were performed as previously described [37]. Survival curves were plotted using PRISM software, and comparisons in survival were calculated using the log-rank Mantel–Cox test and Gehan–Breslow–Wilcoxon test.

RESULTS

General traits and genomic analyses of strains Ab242, Ab244 and Ab825

Ab242, Ab244 and Ab825 (Table 1) are epidemiologically related MDR *Aba* strains obtained from inpatients hospitalized in HECA, Rosario, Argentina [27]. The three strains were subjected to WGS and subsequent analysis of the sequencing data, and a summary of the general genomic features of each of these strains is provided also in Table 1.

WGS analyses indicated that the Ab242, Ab244 and Ab825 genomes were 4 000 608, 3 943 341 and 3 900 868 bp in length, respectively, with a G+C content of 39.1–39.2% (Table 1). The obtained sizes and G+C contents therefore matched the reported averages for the genomes of the *Acinetobacter* spp., i.e. 3.87 Mb and 39.6%, respectively [12]. Each of these strains contains only one chromosome, and house one to three plasmids depending on each strain as judged by the WGS analysis (Table 1).

The assignments of STs following the Oxford (ST^O) or Pasteur (ST^P) MLST schemes [21] were done using the sequences of housekeeping genes derived from the WGS data . These comparisons assigned, in the Oxford scheme, Ab244 and Ab242 both to $ST104^O$ and Ab825 to $ST692^O$ (Table S2). Since $ST692^O$ and $ST104^O$ differ only in the sequence of the *gpi* allele (Table S2), all strains were ascribed to the $CC104^O$ [21]. In turn, all of the above strains shared the same allelic profile in the Pasteur scheme, $ST15^P$, thus conforming the $CC15^P$ (Table S2). These assignments are thus in full agreement with the equivalence between the two *Aba* MLST schemes [21]. A detailed analysis of the MLST database revealed that almost 78% (49/63) of the strains assigned to $CC104^O$/$CC15^P$ were isolated in South America (Table S2). This CC has received lower attention as compared to the main *Aba* CC1 and CC2, but it has been associated to the dissemination of CHDL genes including bla_{OXA-23}, bla_{OXA-58} and $bla_{OXA-143}$ not only in South America but also in a number of European and Asian countries [21, 38, 39]. Moreover, to our knowledge no WGS comparative analysis of $CC104^O$/$CC15^P$ strains has been reported to date.

Comparative analysis of Ab242, Ab244 and Ab825 chromosomes

A comparative analysis was next performed among the chromosomes of strains Ab242, Ab244 and Ab825 (Fig. 1). Other *Aba* chromosomes included in these comparisons were those of the reference clinical strain ATCC17978 [40] and the pre-antibiotic era environmental strain DSM30011 [23]. The two latter strains are generally susceptible to most antimicrobials and were isolated by the middle of last century [23], thus providing a frame for the evaluation of major genome rearrangements among the strains under study. As seen in Fig. 1, a general shared synteny was found between all of the chromosomes of the analysed *Aba* strains, except for five regions including: (1) a Ph prophage region (Ph-A) common to Ab825 and Ab242 (Ph-825-A and Ph-242-A, respectively), although the location of insertion in the chromosome of each of these strains was different; (2) a Tn*6018*-like element common to Ab242, Ab244, Ab825 and also to DSM30011, but inserted in a different chromosomal position in each of the $CC104^O$/$CC15^P$ strains and positioned in an inverted orientation in the DSM30011 chromosome; (3) a similar RI interrupting a tRNA dyhidrouridine synthase gene (*dusA*) present in Ab244 and DSM30011; (4) a second copy of a Tn*6022* located in a different chromosome location in Ab825; and (5) a Tn*10* element carrying tetracycline resistance determinants also in Ab825 only (see below for details).
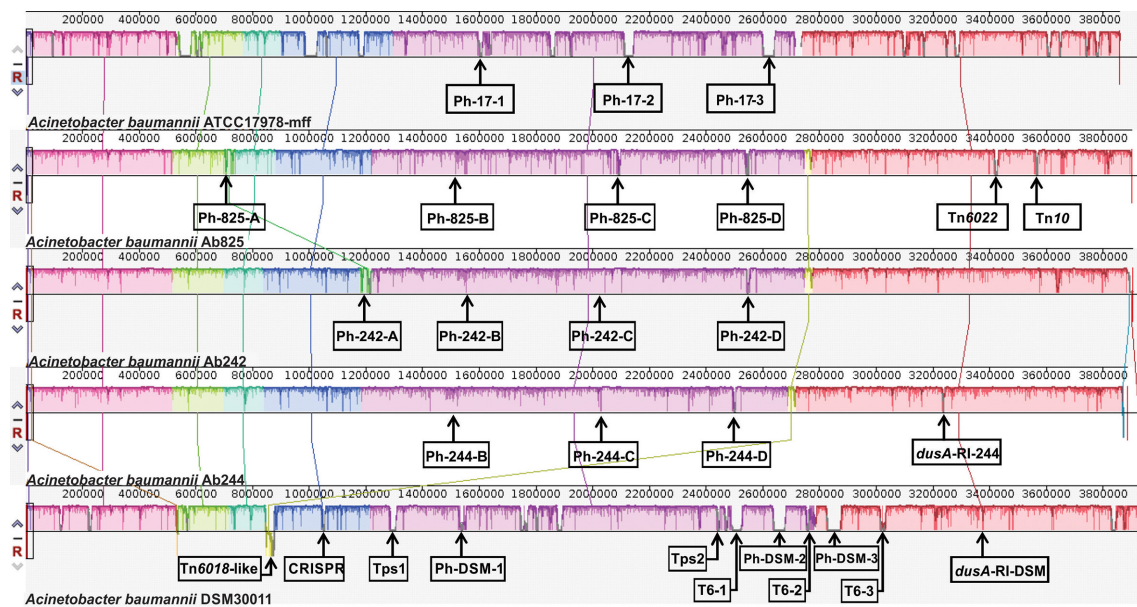
Fig. 1. Linear comparison of the genomes of *A. baumannii* strains ATCC17978, Ab825, Ab242, Ab244 and DSM30011 inferred using Mauve. Each block corresponds to a DNA fragment of the chromosome and is distinctively coloured for clarity. The degree of conservation is indicated by the vertical bars inside the blocks. Their position relative to the genome line denotes co-linear and inverted regions. Putative prophages (Ph/strain-number; seeTable 3 for details) are displayed for all strains. Two regions usually associated with antimicrobials resistance (Tn*6022* and Tn*10*) are shown for strain Ab825 (see text for details). Regions encoding a Tn*6018*-like element, a CRISPR-cas cluster, two-partner systems (Tps-1 and 2) and type-6 secretion-system-related genes (T6-1 to 3) are indicated for DSM30011 genome [23]. A resistance island inserted into the *dusA* gene is present in Ab244 and DSM30011 chromosomes.

It is worth noting the conspicuous absence in all three CC104^O/CC15^P strains of gene clusters encoding defensive mechanisms against biological aggressors such as: (1) genes associated to type-6 secretion systems (T6SS). In contrast, a complete T6SS main cluster and several toxin-encoding genomic islands are present in each of the ATCC17978 and DSM30011 chromosomes [37, 41]; (2) a CRISPR-cas anti-phage system, which is missing also in ATCC17978 but is present in DSM30011 [37]; (3) contact-dependent inhibition (CDI) type 5 secretion systems (T5SS) of the Two-partner system (Tps) subclass [42], absent in ATCC17978 as well. Remarkably, two different T5SS clusters are present in the DSM30011 chromosome (locus tag DSM30011_05955–60 and locus tag DSM30011_11640–45, respectively) [43] probably reflecting the environmental origin of this strain and the concomitant selection pressures [23].

Resistance islands

Aba RI are important vehicles for the accumulation of different antimicrobial (AbaR) and heavy-metal ion-resistance genes [44]. The comparisons of the genomic sequences of 249 *Aba* strains indicated four well-defined hot-spots for AbaR insertions including *comM*, *pho*, *astA*, and an acetyl transferase (acetylT) gene [16]. In Ab242, Ab244 and Ab825 chromosomes (Fig. 2a), the *comM* gene was found interrupted by the insertion of a Tn*6022* composite transposon [45]. Tn*6022* constitutes the basic backbone of AbaR4, a RI in which a Tn*2006* transposon carrying a *bla*$_{OXA-23}$ carbapenemase gene

is inserted, and which is carried mostly by strains of the widely disseminated IC II [45–48]. The observation above that Ab242, Ab244 and Ab825 contain within the *comM* gene a single Tn*6022* element lacking resistance genes and inserted in all cases at an identical site (Fig. 2a) therefore indicated that its acquisition occurred most likely in a common ancestor. Moreover, that carbapenem resistance in Ab242 and Ab825 resulted from other mechanism(s). Of note, in the Tn*6022* element carried by Ab242 a complete IS*Aba125* element was additionally located in the intergenic region between *uspA* and a hypothetical gene (locus tag CJU83_17765), thus suggesting that its acquisition occurred independently in this strain. In addition, a second Tn*6022* copy was found in the Ab825 chromosome (Fig. 1), in this case disrupting an *asnA* L-asparaginase gene (locus tag CLM70_16865) in what constitutes a previously unreported location for this transposon.

Aba strains usually encode diverse gene clusters encoding systems involved in the detoxification of noxious compounds [49]. Interestingly, the three strains studied here carry a Tn*6018*-like transposon inserted in all of them at the same genomic position and carrying resistance genes to heavy-metal ions (Table 2). This element was previously identified in a reduced number of *Aba* strains isolated from the environment (DSM30011) and also from the clinical setting (AB031 and ATCC19606) [23]. This RI, which is missing in strain ATCC17978, is located in a different genomic locus and
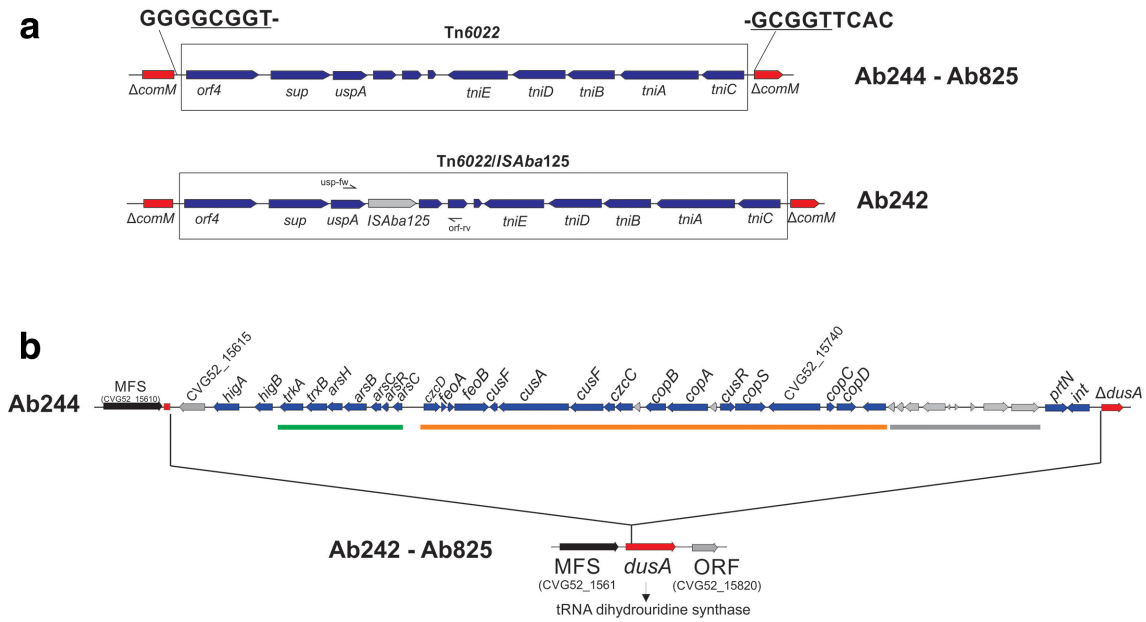
Fig. 2. Schematic representations of the genomic islands interrupting *comM* and *dusA* in the *A. baumannii* clinical strains under study. (a) Tn*6022* elements found interrupting the *comM* gene in the three strains under study (see Table 2 for details). The direct repeat generated at the site of integration is shown enlarged and underlined. In the Tn*6022* element found in Ab242, an additional IS*Aba125* element was localized downstream of the *uspA* gene. The sites of hybridization of the pair of primers (see Table S1) employed to corroborate this insertion by PCR amplification analysis is shown. (b) Genomic island interrupting the *dusA* gene in the Ab244 strain (see Table 2 for details). Copper and arsenic ion-resistance clusters are underlined by green and orange bars, respectively. Genes encoding hypothetical phage proteins (grey arrows) are underlined by a grey bar. For comparisons, the intact *dusA* gene and its flanking genes found in the chromosomes of both Ab242 and Ab825 strains are shown below.

in an opposite orientation in the DSM30011 chromosome (Fig. 1). We previously reported [23] the presence of a 33 kbp RI encoding resistance to heavy-metal ions in DSM30011 interrupting the *dusA* gene (DSM30011_16220). This spot represents a common integration site for this kind of genetic element in *Aba* [49, 50]. The RI identified in DSM30011

includes arsenate and heavy-metal-ion detoxification systems such as *ars*, *czc* and *cop*, as well as genes putatively involved in iron ion transport (*feoAB*) [23]. A similar region was also detected at the Ab244 *dusA* locus (Fig. 2B and Table 2). Interestingly, this RI contains three additional genes, two of them encoding a HigAB toxin-antitoxin module [49, 50], and the

Table 2. Resistance islands

Toxic compounds- Resistance islands							
Name	**Strain**	**Position (bp)**	**Length (kb)**	**Integrase locus tag**	**Integration site**	**Upstream of integration site locus tag**	**Downstream locus tag**
Tn*6018*-like	Ab242	2742324–2778290	36.0	CJU83_13560	tRNA-Ser-TGA	CJU83_13360 NLPA lipoprotein	CJU83_13570 2,4-dienoyl-CoA reductase
	Ab244	2683153–2719121	36.0	CVG52_13180		CVG52_12975 NPLA lipoprotein	CVG52_13190 2,4-dienoyl-CoA reductase
	Ab825	2739913–2776075	36.1	CLM70_13810		CLM70_13610 NPLA lipoprotein	CLM70_13820 2,4-dienoyl-CoA reductase
	DSM 30011	843472–874327	30.8	DSM30011_04155		DSM30011_03930 transcription elongation factor GreB	DSM30011_04160 SgcJ/EcaC family oxidoreductase
***dusA*-RI**	Ab244	3233058–3273869	40.8	CVG52_15810	*dusA*	CVG52_15610 MFS transporter	CVG52_15820

Table 3. Putative prophages*

Strain	Name	Length (kb)	Nucleotide position (bp)	Integrase locus tag	Integration site	Upstream locus tag	Downstream locus tag
Ab242	Ph-242-A	48.5	1174360–1222933	CJU83_05530	tRNA-pseudo-Arg-CCG	CJU83_05525 ABC type transporter	CJU83_05880 hypothetical protein
	Ph-242-B	53.6	1519370–1573046	CJU83_07300	IR† (hypothetical protein-MFS transporter)	CJU83_07295 hypothetical protein	CJU83_07715 MFS Transporter
	Ph-242-C	30.6	2076444–2107079	CJU83_10280	IR† (malG-zapE)	CJU83_10090 Malate synthase G	CJU83_10285 ZapE (cell division protein)
	Ph-242-D	43.5	2540407–2583982	CJU83_12385	tRNA-Gly-GCC	CJU83_12375 cysteine-tRNA ligase	CJU83_12630 hypothetical protein
Ab244	Ph-244-B	53.7	1476585–1530289	CVG52_06995	IR (hypothetical protein-MFS transporter)	CVG52_06990 hypothetical protein	CVG52_07415 MFS transporter
	Ph-244-C	29.2	2027692–2056979	CVG52_09970	IR (*malG-zapE*)	CVG52_09790 Malate synthase G	CVG52_09975 ZapE (cell division protein)
	Ph-244-D	33.3	2488724–2522040	CVG52_12065	tRNA-Gly-GCC	CVG52_12055 cysteine-tRNA ligase	CVG52_12250 hypothetical protein
Ab825	Ph-825-A	54.6	718987–773665	CLM70_03610	tRNA-Arg-CCT	CLM70_03370 HchA, protein deglycase	CLM70_03985 Aminoacid permease
	Ph-825-B	62.3	1546982–1609384	CLM70_07550	IR (hypothetical protein-MFS transporter)	CLM70_07545 hypothetical protein	CLM70_08115 MFS transporter
	Ph-825-C	41.3	2100618–2141947	CLM70_10600	IR (*malG-zapE*)	CLM70_10350 Malate synthase G	CLM70_10605 ZapE (cell division protein)
	Ph-825-D	40.3	2573757–2614071	CLM70_12695	tRNA-Gly-GCC	CLM70_12685 cysteine-tRNA ligase	CLM70_12885 hypothetical protein

*According to PHASTER predictions.
†IR; intergenic region.

other a Beta protein, which acts as an antitoxin of the Gop toxin that prevents host cell killing by the T4 bacteriophage [51]. These genes may serve to stabilize this RI in the Ab244 genome in cells transiting under non-selective environments.

Mobile genetic elements in Ab242, Ab244 and Ab825 genomes

Prophages

Bacteriophages provide a source of genomic variability in *Aba* [52]. The prediction of bacteriophage sequences in the clinical strains analysed here uncovered the presence of four prophages in the chromosomes of each Ab242 and Ab825, and three in Table 3 Ab244. Prophages inserted at the same chromosomal location in the three strains (i.e. Ph-B, C and D, Fig. 1, Table S3) showed nucleotide identities higher than 99% and identical sequences for hallmark genes such as integrase, terminase, as well as for phage capsids and tails. Moreover, their integration sites are in concordance with previously reported hot-spots for phage integration in the *Aba* chromosome [16]. In contrast, prophages Ph-242-A and Ph-825-A, which were located only in strains Ab242 and Ab825, displayed

different integration sites in the corresponding chromosomes (Fig. 1). From them, Ph-825-A was found in a tRNA-Arg gene (Table 3), an integration site already described in other *Aba* strains [16]. Ph-242-A, in turn, was also found inserted into a tRNA-Arg gene located in a different chromosome region when compared to Ph-825-A. In addition, Ph-242-A insertion generated a 15 bp-deletion at the 3′-end of the target tRNA-Arg gene (Table 3).

Further bioinformatic analysis indicated that, with the only exception of Ph-244-D, all of the other prophage sequences described above encode for complete prophage components (Table S3).

Insertion sequences

The identity and number of IS copies present in the genomes of Ab242, Ab244 and Ab825 was predicted by bioinformatic analysis (Table S4), and the inferred ISs were then manually curated. Remarkably, the Ab825 genome contains the larger variety and number of ISs with a total of 44, whereas only 14 and 11 IS copies were found in Ab242 and Ab244, respectively.

Table 4. Insertion sequence content of the *A. baumannii* strains under study*

Location	IS type	Strain		
		Ab242	**Ab244**	**Ab825**
Chromosomal contigs	IS*Aba125*	1	1	11
	IS*10*	–	–	9
	IS*Aba43*	1	–	6
	IS*Aba31*	2	2	3
	IS*Aba42*	1	1	3
	IS*Aba1*	–	1	3
	IS*Aba26*	1	1	1
	IS*Aba825*	–	–	1
	IS*our*	1	2	–
	IS*Vsa3*	1	1	–
	IS*15DII*	–	1	–
Complete plasmids†	IS*Aba125*	2	–	2
	IS*26*	1	1	2
	IS*Aba3*	2‡	–	2‡
	IS*Aba825*	1	–	1
	Total	14	11	44

*Based on IS Finder annotation.
†See Table 1.
‡One incomplete copy.

Not only the number of ISs found in Ab825 is significantly higher than the reported average of 33 copies per *Aba* genome [19], but the diversity of IS families found in this genome is also high as well (Table S4). The most abundant IS elements found in the three *Aba* genomes analysed are intrinsic to the *Acinetobacter* genus (IS*Aba*-type) and are generally present in multiple copies [19]. Among them the most prevalent is IS*Aba125*, with 13 copies scattered throughout the whole Ab825 genome (Table 4).

Of note, two novel ISs one of 1320 bp and the other of 2655 bp, were identified in the genomes of the clinical strains under study, and the corresponding sequences were submitted to the ISSaga database from ISfinder [32]. These new ISs were assigned the designations IS*Aba42* and IS*Aba43*, respectively (Fig. S1). IS*Aba42* belongs to the IS*256* family, and IS*Aba43* to the ISL3 family. IS*Aba42* carries a transposase gene encoding a protein of 403 amino acids with a 95% of similarity to the ISEc39 transposase (CP001855) including a typical MULE domain [53] associated to *Escherichia coli* strain S43 [54]. IR-R and IR-L inverted repeats of 24/28 bp at the ends of IS*Aba42* were identified, as well as a 8 bp direct repeat (DR) at the site of insertion (Fig. S1). IS*Aba42* was only detected in the *Acinetobacter* sp. ACNIH1 plasmid pACI-3bd5 and in the chromosome of *Acinetobacter* sp. NCu2D-2. Remarkably,

this IS was found interrupting a RTX-family toxin gene in the three analysed strains (see below).

In the case of IS*Aba43*, six copies were found in the chromosome of strain Ab825 and only one in Ab242. IS*Aba43* bears two genes, the first encoding a drug resistance transporter of the Bcr/CflA subfamily (421 aa) and the second a DDE transposase (401 aa) displaying 69% amino acid identity with the IS*Aeme19* transposase [55]. The IR-R and IR-L inverted repeats of this IS are 65 bp long each, and its insertion generated a direct repeat (DR) of 8–10 bp in length at the target site (Fig. S1). IS*Aba43* is present in the other 19 strains of the *Acinetobacter* genus.

It is worth noting that IS*Aba43* is the third in prevalence (*n*=6; Table 4) in strain Ab825, indicating a relatively relevant role in the remodelling of this genome.

Plasmids
Plasmids are the most frequent vehicles directly implicated in the acquisition of AR resulting from lateral gene transfer both intra- and inter-species [56]. Ab242 strain contains three plasmids (pAb242_9, pAb242_12, and pAb242_25) [57], Ab825 strain contains two plasmids (pAb825_36 and pAb825_12), and the carbapenem-susceptible (Carb^S) Ab244 strain houses only a single plasmid (pAb244_7) (Table 1).

Ab242 and Ab825 strains display clinical resistance to carbapenem β-lactams including imipenem and meropenem (Table S5). The source of carbapenem resistance in these two strains is the presence of similar Rep-3 resistance plasmids (pAb242_25 and pAb825_36) containing identical adaptive modules of ~9.5 kbp carrying a bla_{OXA-58} gene within a defective Tn3, and in which the insertion of an IS*Aba825* in the IS*Aba3* copy located upstream of bla_{OXA-58} resulted in its overexpression [9, 57]. In addition, this adaptive module also encompasses a Tn*aphA6* composite transposon inserted downstream of the bla_{OXA-58} gene and conferring amikacin resistance to the *Acinetobacter* host (Table S5) [57]. Of note, the module is bordered by several sites potentially recognized by the XerC/D site-specific tyrosine recombinases of the host (XerC/D-sites) [57]. Moreover, we recently demonstrated that some XerC/D-sites present in Ab242 plasmids can actually constitute active pairs proficient for site-specific recombination (SSR) mediating plasmid fusions and resolutions, and postulated that these and subsequent structural rearrangements may facilitate the dissemination of resistance structures bordered by XerC/D-sites [57].

In the above context, comparative sequence analysis between pAb244_7 (Fig. S2) housed by Ab244 and Ab242 plasmids [57] revealed an extensive sequence identity between pAb244_7 and pAb242_9 (from the latter strain) also lacking AR genes (Fig. S3). pAb244_7 has a length of 7965 bp and contains 13 ORFs, and none of them encoding antimicrobial resistant determinants (Fig. S2). The main difference between these two plasmids is the additional presence of an approximately 1.3 kbp region in pAb242_9 carrying a *relBE* toxin-antitoxin system and a *fdx* (ferredoxin) gene (Fig. S3). Of note, this region is also bordered by two directly oriented

XerC/D-sites designated no. 14 and no. 16, respectively (Fig. S3). The presence of a XerC/D-site in an equivalent position in pAb244_7 (no. 14) strongly suggests that the acquisition of this 1.3 kbp fragment by pAb242_9 was also the consequence of structural rearrangements subsequent to a SSR event mediated by the XerC/D system. XerC/D-sites present in *Acinetobacter* plasmids have in fact been implicated in the acquisition of different modular structures including not only AR genes but also toxin-antitoxin (TA) systems, heavy-metal-ion resistance genes, etc [18, 57–59]. The observations of this work thus provide further clues on the contribution of XerC/D-mediated SSR events to the structural remodelling of *Aba* plasmids and the dissemination of modular structures bordered by these sites.

Antimicrobial resistance differences between Ab244, Ab242 and Ab825 strains can be attributed to differences in resistance genes' repertoire or expression

The three analysed strains exhibited resistance to different β-lactams, except for carbapenems, and extended spectrum cephalosporins, quinolones and aminoglycosides (Table S5), thus classifying as MDR. The carbapenem and amikacin resistance phenotypes of Ab242 and Ab825 could be attributed to a plasmid-borne bla_{OXA-58} and *aphA6* genes, respectively. However, the resistance to β-lactams such as ampicillin and cephalosporins, and differential levels of resistance to other antimicrobial classes such as folate synthesis inhibitors and tetracycline (Table S5) prompted us to perform bioinformatic predictions of the antimicrobial gene repertoire in the genome of the studied strains (Table S6). The resistance to ampicillin displayed by the three strains (Table S5) most likely reflects the contribution of different β-lactamase genes in the corresponding chromosomes including bla_{OXA-51} and bla_{ADC-25} (encoding a AmpC-type β-lactamase) in all of them, and a $bla_{TEM-1-B}$ in Ab244 (Table S6). The chromosomal bla_{OXA-51} gene is intrinsic to *Aba* and a hallmark of this bacterial species [60]. The insertion of ISs upstream bla_{OXA-51} generating strong promoters is the cause of Carb^R phenotypes [61], but this was not the case of the strains analysed here (Table S6). This reinforced the above notion that carbapenem resistance in Ab242 and Ab825 resulted from the acquisition of the bla_{OXA-58} plasmid-borne gene. In addition, *Aba* carries a chromosomally encoded AmpC-type bla_{ADC-25} β-lactamase, and the over-expression of this gene resulting from the upstream insertion of IS*Aba1* elements providing a strong promoter has been associated to increased cephalosporin resistance [62, 63]. All of the *Aba* clinical strains analysed here showed resistance to different cephalosporins, with Ab242 showing lower (intermediate) resistance to ceftazidime and cefepime when compared to either Ab244 or Ab825 (Table S5). The higher levels of resistance to these two cephalosporins shown by the two latter strains could be thus attributed to the presence of an IS*Aba1* copy upstream of bla_{ADC-25} in the corresponding chromosomes (Table S6). Regarding resistance to folate synthesis inhibitors (sulfamethoxazole/trimethoprim) shown by Ab242 and Ab244 (Table S5), these resistance profiles are in concordance with the presence of the *sul2* gene in both strains (CJU83_19430 and CVG52_19110, respectively)

[64, 65]. The susceptibility phenotype displayed by Ab825 (Table S5) represents a notable exception when compared to their genetically related strains as well as to other *Aba* clinical strains [5, 15, 66, 67]. This could be associated to the interruption of the use of these drugs to treat bacterial infections [68]. In turn, the tetracycline-resistant phenotype of Ab825 as compared to the other two strains (Table S5), likely reflects the presence of a Tn*10* composite transposon [69] in this strain (Table 2 and Table S6). This transposon, possesses a total of eight genes [four of which have role(s) in tetracycline resistance], and was found inserted in the Ab825 chromosome in the intergenic region between a serine hydrolase gene (CLM70_17480) and a *merR* transcriptional regulator (CLM70_17535). The fact that this region is intact in both the Ab242 and Ab244 chromosomes suggests that this mobile element was independently acquired by Ab825.

Comparative analysis of the virulence potential of the analysed *A. baumannii* clinical strains using the *G. mellonella* larvae insect model

G. mellonella larvae provide us with a reliable model to evaluate/compare the pathogenicity of different *Aba* strains [41, 70]. In the case of the different clinical strains analysed, and in comparison with ATCC 17978 used as an *Aba* reference strain, we observed that both Ab244 and Ab242 were significantly less virulent than ATCC17978 at a dose of 10^6 c.f.u. (Fig. 3a). In contrast, the killing of the larvae was abrupt when Ab825 was assayed at this bacterial load dose indicating a higher virulence for this strain to allow any comparison of virulence (not shown). In fact, when the injected Ab825 bacterial load was lowered tenfold to 10^5 c.f.u. (Fig. 3b), we consistently observed that this strain killed more efficiently the larvae than all of the other strains tested, including ATCC17978 (Fig. 3b) and Ab242 and Ab244, which for clarity were not included in the figure.

Identification of persistence and virulence determinants among the analysed *A. baumannii* strains

Next, we aimed to determine the genomic features that could explain the significant differences in virulence shown above by the analysed strains. Initial homology searches using as queries genes encoding virulence factors [13, 22, 71] over the genomes of the three *Aba* strains indicated the presence of most of them (Table S7). Some particular cases are hereafter described:

(i) Exopolysaccharides (EPS). Surface polysaccharides play a very important role in *Aba* pathogenesis [72]. EPS produced by *Aba* include a capsule and a short version of the lipopolysaccharide O-antigen [73, 74], both of which are exposed in the cell surface and are highly immunogenic. However, the composition and structure of both K and O antigens vary considerably between strains, and these differences can substantially modify recognition by host defenses [75]. Our analysis indicated that the K-loci identified in the three MDR strains displayed similar genetic organization, which corresponds to that denominated PSgc12 in the classification of Hu *et al.* [75] (Fig. S4). A distinctive feature,
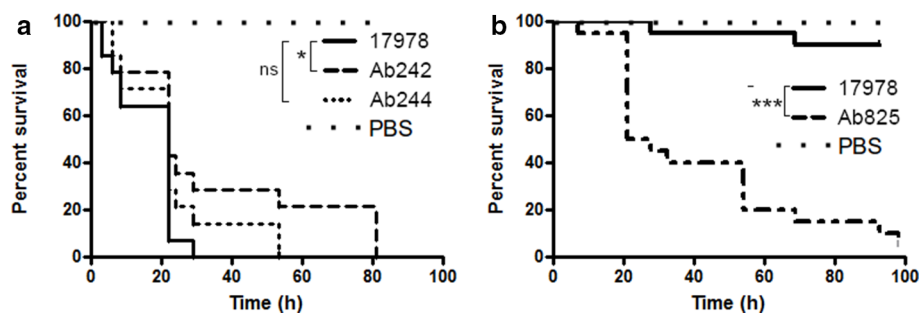
Fig. 3. *G. mellonella* lethality assays of the different *A. baumannii* strains under study. (a) Comparative survival analysis of *G. mellonella* larvae injected with 10^6 c.f.u. doses of Ab242 or Ab244 strains. The same dose of the *Aba* ATCC17978 was also tested as a control reference strain (*$P<0.05$; n.s.: non-significant). PBS was used as a control. (b) Same, but employing 10^5 c.f.u. doses of Ab825 or ATCC17978. (***$P<0.0001$). In all cases the data are representative of three separate survival experiments, each performed with 20 larvae. Survival curves were constructed by the Kaplan–Meier method and compared by Log-rank analysis.

is the interruption of the *cgmA* gene located between the *pgm* (encoding a phosphoglucomutase) and the *gne* genes (encoding a UDP-NAc-glucose-4-epimerase) by an IS*Aba31* element (Table S7, Fig. S4). Domain-search analysis indicated that *cgmA* encodes a hypothetical protein carrying a lipoteichoic acid synthase like domain (cd16015). Notably, and despite the fact that lipoteichoic acids have not been described among Gram-negative bacteria, this gene is widely distributed in both environmental and clinical isolates of *Aba* [23, 75]. Still, any potential role of *cgmA* in the capsule synthesis process remains to be determined, and whether its absence confers some selective advantages in the clinical environment. Moreover, an IS*Aba26* element was detected in the intergenic region between *cgmA* and *gne* (Fig. S4).

The detailed analysis of the nucleotide sequences revealed interesting differences between the K-locus of the analysed strains. Firstly, strain Ab825 contains a different variation of the *wzx* gene. Wzx is in charge of translocating the short oligosaccharide repeat units across the inner membrane and into the periplasm [74]. There is a large sequence polymorphism between *Aba* Wzx proteins [48, 75], and it is widely accepted that these proteins possess significant substrate specificity, mainly involving the recognition of the first sugar in the repeat unit and also the presence of a side branch [76]. Consequently, the identification of a different *wzx* allele in Ab825 suggests that the basic oligosaccharide repeat unit in its capsule may differ from that of Ab242 and Ab244. In concordance with this hypothesis, the *wagG* and *wagH* genes predicted to code for proteins with sugar-branching activity (Fig. S4, Table S7), are only present in the Ab825 strain.

We then analysed the organization of the OC-locus. Twelve different OC-loci (namely OCL1-OCL12) have been defined on the basis of aminoacid sequence similarity analysis of more than 200 *Aba* strains [77]. A similar search revealed that each of the three strains analysed possess an OCL7-type locus. These loci displayed comparable gene contents (Table S7) encoding each five different glycosyl transferases, one polysaccharide deacetylase, three hypothetical proteins and one protein carrying a hydrolase domain.

(ii) Iron uptake. Since the ability to acquire iron from the host contributes to *Aba* virulence [78–80], we analysed the occurrence of different iron-uptake systems in the MDR strains. However, all of them showed five different clusters involved in the acquisition of iron ions (Table S7), including a *feo*ABC cluster responsible for the active uptake of Fe(II) [36]; the acinetobactin cluster directing the synthesis of a widely characterized siderophore displaying a major role in Fe(III) ion scavenging [81]; two additional clusters involved in heme uptake (heme-uptake clusters 2 and 3) [36, 82], and a baumanoferrin gene cluster responsible of the synthesizes of a hydroxamate-type siderophore [36, 83]. To obtain clues on the distribution of the above iron acquisition systems in the general *Aba* population, we conducted genomic comparative analyses on 128 *Aba* clinical strains and three of environmental origin, DS002, DSM30011 and NCIMB8209 [23, 24], thus totalizing 132 publicly available genomes. We determined the presence of the five iron-uptake clusters mentioned above in 72 (54.5%) of the above genomes. Remarkably, 57 (43.2%) of the remaining strains carry four of these clusters, only lacking the heme-uptake cluster 3. Notably, this cluster is also absent from *Aba* environmental strains DSM30011 and NCIMB8209 [23]. It is also worth mentioning that *Aba* DS002, only carry three iron-uptake clusters [24], lacking acinetobactin as well as the heme-uptake cluster 3 [24]. The presence of the five iron-uptake systems in the Ab242, Ab244 and Ab825 strains reinforced the idea that their presence most probably contributed to the adaptation of *Aba* to the clinical environment [80].

(iii) CpaA. The *cpaA* gene encodes a metallopeptidase exhibiting the ability to cleave fibrinogen and coagulation factor XII, thus helping deregulate blood coagulation during infection [84]. CpaA, a substrate of the type-II secretion system, was thus proposed as a *bona fide* virulence factor [13, 85]. Our analysis indicated that all three strains lack the *cpaA* gene. In this context, the analysis of *cpaA* presence among the aforementioned genomes of 132 *Aba* strains showed that only 17 (12.9%) carry this gene. Interestingly, six of them belong to ST10^P and another three to ST23^P. This indicates that this virulence gene is not broadly distributed in *Aba*
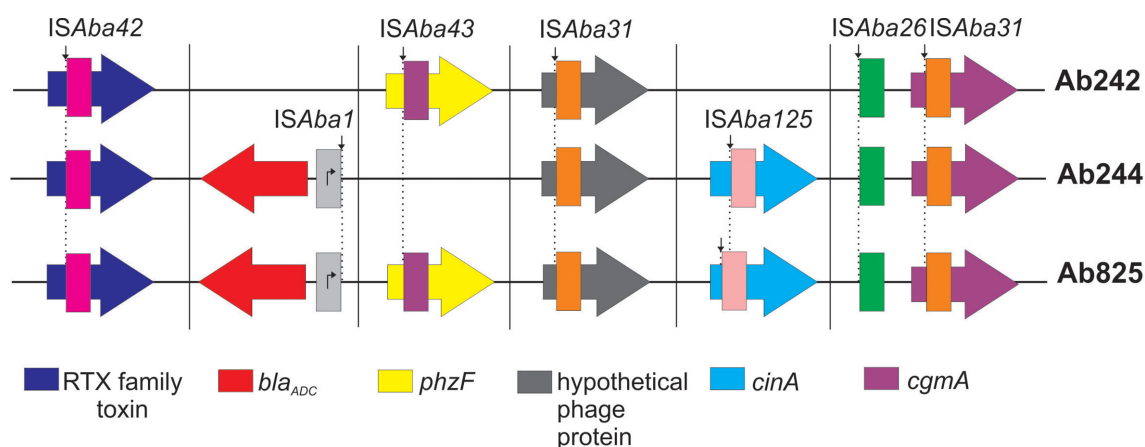
Fig. 4. Schematic representation of the chromosomal location of ISs shared among Ab242, 244 and Ab825 strains. The IS positions are schematically depicted according to their location in the corresponding genomic sequence (Table S8). IS*Aba42* (magenta), IS*Aba43* (purple), IS*Aba31* (orange), IS*Aba125* (pink) and IS*Aba26* (green) interrupt different target genes whereas IS*Aba1* (light grey) falls in an intergenic region upstream of *bla*~ADC~ gene (red arrow). Thus generating a strong promoter putatively enhancing the expression of this resistance gene. The IS insertion sites in a given target gene were depicted with a vertical black arrow and dashed lines. Genes are not drawn to scale.

clinical isolates, and suggests that its presence is restricted to some clonal lineages.

Insertion sites of IS elements in the chromosomes of the *A. baumannii* strains under study

The above observations prompted us to investigate other genetic variations over the Ab825 genome. IS elements are important drivers of genomic rearrangements in *Aba* clinical strains [19, 44]. Our analysis detected that some IS shared the same chromosomal insertion site between the three strains under study, as in the case of IS*Aba42* disrupting a gene encoding a type-I secretion-system-dependent protein, which probably functions as a RTX family toxin mediating biofilm development [86]; IS*Aba31* interrupting a gene for a putative phage protein, as well as the *cgmA* gene mentioned above (Fig. 4, Table S8). The insertional inactivation of any of the above three genes had not been reported previously in other *Aba* strains. These observations not only suggest that these three genes were already disrupted by the indicated ISs in a common ancestor of the three CC15^P strains, but also reinforced their close clonal relationship detected by our genomic analysis. A study of 976 *Aba* genomes indeed found that phylogenetically closely related strains show analogous patterns of ISs inserted at equivalent sites in their genomes [19].

Other IS integration events involved two out of the three strains under study. In this context, we mentioned above the IS*Aba1* copy located at the same position upstream of the *bla*~ADC~ gene in Ab244 and Ab825 (Fig. 4, Table S8). Furthermore, a IS*Aba43* copy was found in Ab242 and Ab825 disrupting a gene encoding a PhzF-like protein [87] of unknown function (Fig. 4, Table S8). Moreover, a putative nicotinamide mononucleotide deamidase *cinA* gene implicated in competence [88], was interrupted by *ISAba125* in both Ab244 and Ab825

(Fig. 4, Table S8). In this case, however, this IS was inserted at different locations within *cinA*, thus indicating independent acquisitions by each of these strains (Fig. 4). The IS-mediated inactivation of *cinA* has already been documented in at least 30 *Aba* genomes [19], although the physiological effects of these disruptions are unknown.

This bioinformatic analysis identified 16 IS-mediated gene disruptions in the Ab825 chromosome (Table S8). Some of the interrupted genes participate in biofilm formation and attachment to abiotic surfaces such as *pgaB* involved in the synthesis of poly-*β*-(1-6)-*N*-acetylglucosamine PGA exopolysaccharide, *csuA* encoding a Csu pilus subunit, and a di-guanylate cyclase gene regulating biofilm production [2, 5, 89, 90]. In addition, an IS*Aba1* was found at the intergenic region between the CsuA/B component and a TetR-family transcriptional regulator (Table S8). Multiple IS integration events within the *Aba csu* cluster have been reported in clinical isolates [19], and the loss of the Csu pilus has been linked to niche specialization due to either increased invasiveness or enhanced survival [16]. It is therefore tempting to speculate that these IS-mediated disruption events may explain the only modest capacity of Ab825 strain to form biofilm and to adhere to both plastic surfaces and cultured epithelial lung cells [37].

Other genes encoding putative *Aba* virulence factors, such as a phospholipase D involved in host colonization [91] and the AsaA structural component of the T6SS [41, 92, 93] are also inactivated by IS*Aba125* elements in Ab825 (Table S8). Regarding the latter, we have previously demonstrated that Ab825 lacks a functional T6SS [37]. Of note, losses of T6SS main cluster genes have been previously reported in particular clonal lineages of phylogenetically and epidemiologically related *Aba* clinical MDR strains [26, 94, 95]. T6SS participates in interbacterial competition and may also have roles

in host colonization, as judged by *G. mellonella* larvae model infection assays [37, 96]. However, the loss of this system in Ab825 and other MDR clinical strains suggests that it may not be critical for bacterial survival in the conditions prevailing in the nosocomial environment. Furthermore, silencing of the T6SS was recently shown to be critical for HGT through conjugation, which is crucial for AR spread [97]

Another gene disrupted by IS*Aba825* in strain Ab825 is *carO*, which codes for the second most abundant *β*-barrel protein after OmpA of the *Aba* outer membrane [10] (Table S8). CarO participates in the permeation of carbapenems across the OM [6, 7, 10], and has been proposed to also play roles in *Aba* pathogenicity [7, 8]. CarO enhances *Aba* cell adhesion and nasal colonization in mice mainly by inhibiting host inflammatory responses [98]. Other genes found disrupted by ISs in Ab825 are those encoding a ribonuclease D and a sensor histidine kinase (Table S8). The IS-mediated disruptions of these genes in other *Aba* strains have been previously described [19], but the physiological effects of these losses are hitherto unknown.

Not all IS insertions selected in the Ab825 chromosome are necessarily gene disruptive. In fact, some ISs confined to intergenic regions (Table S8) may have enhancing effects on the expression of adjacent genes. In this regard, it has been shown that IS*Aba1*, IS*Aba125* and IS*Aba825* have strong outward-facing promoters, and that their insertions up-regulate the expression of proximal genes in *Aba* as in the cases of several *β*-lactamases [9, 17, 57, 61] and catalases [20]. In fact, this is most likely the situation resulting from the insertion of IS*Aba1* upstream of the chromosomal bla_{ADC-25} gene (Fig. 4, Table S8) thus conferring cephalosporin resistance to the host; and IS*Aba825* upstream of the plasmid-borne bla_{OXA-58} gene in Ab242 and Ab825 thus conferring carbapenem resistance. Whether other IS insertions at IRs in the Ab825 chromosome were selected due to abolishing or enhancing expression of adjacent genes, and the possible effects on the pathophysiology of *Aba*, remain to be established.

DISCUSSION

MDR *Aba* nosocomial infections have become a public health concern, with a pan-drug resistance scenario emerging in the horizon as a worrying threat [2, 3, 5, 11]. Rapid acquisition of additional drug resistance is considered a main determinant of the success of *Aba* strains in the nosocomial environment [2, 3, 5]. The *Aba* virulence potential in turn seems intrinsic to the species, with the clinical outcomes depending on multiple host–bacterial interactions [3]. Different epidemic strains may in fact use distinct combinations of virulence determinants to optimize adaptation to the human host [2]. In this context, WGS comparisons represents a powerful tool to analyse these strategies.

Here, we conducted WGS comparative analysis of three clonally and epidemiologically related MDR strains belonging

to the CC104[O]/CC15[P], a CC linked to the dissemination of different CHDL genes in South America and some European and Asian countries [21, 99, 100]. Expectedly from their close relationships a general shared synteny was found between the chromosomes of all of these strains. Still, a more detailed analysis uncovered a number of acquired traits that contributed to genetic variability between strains, among them a heavy-metal ions RI only in Ab244, and a Ph-A prophage common to Ab242 and Ab825 but absent in Ab244. Furthermore, a search for AR genes revealed different repertoires carried in the chromosome or in plasmids. The most relevant are those conferring resistance to carbapenems and aminoglycosides genes, embedded in an adaptive module carried by plasmids present in Ab242 and Ab825 [57]. Their acquisition certainly contributed to the adaptation of the studied strains to the hospital environment when imipenem therapy was implemented [27]. It is worth noting the presence in all strains hereby analysed of an intact Tn*6022* copy disrupting the *comM* gene. This represents the common insertion site for this element in many *Aba* genomes, and provides a hot spot for the integration of additional MGE carrying different resistance genes which turn this region into a *bona fide* RI [16, 45]. Intriguingly, Ab825 contains a second intact copy of Tn*6022* disrupting a *asnA* gene in an unreported chromosomal location for this transposon. In contrast, resistance genes conferring the MDR phenotype are scattered in the genome of these strains, and in some cases the acquisition of a proper resistance phenotype depends more on IS elements than on HGT events as is the case of IS*Aba1* driving overexpression of bla_{ADC-25} in Ab244 and Ab825 resulting in increased cephalosporin resistance.

Another interesting observation is the lack of defense mechanisms against biological aggressors such as CDI, and T6SS CRISPR-cas systems in the strains under study. The loss of these systems by IS inactivation or recombination processes might be beneficial for strain survival in the hospital setting, since it enables dissemination of MGEs such as plasmids [97, 101]. In this context, examination of the strains under study indicated an extensive IS dissemination over the Ab825 genome as compared to Ab242 and Ab244. A total of 44 IS copies were identified in Ab825, which reinforces the idea of their importance in the remodelling of the genome of this particular strain. Inspection of the integration sites showed a conspicuous IS-mediated inactivation of genes involved in the synthesis of surface-exposed structures such as exopolysaccharides, pili, T6SS and OMP such as CarO. These findings are in line with proposals of the pivotal role of the *Aba* envelope in the infection process, since it contributes to protection from external aggressors including antimicrobials, other membrane disrupting substances, and effectors of the innate immune system [22]. In this context, gene inactivation may be important for *Aba* virulence in the form of immune evasion [2, 74], as has been previously determined for this and other bacteria [25]. This could explain infection assays indicating that strain Ab825 shows increased

virulence. In addition, the different gene composition of the Ab825 K-locus responsible for capsule synthesis could also contribute to its higher relative virulence.

Overall, the genetic variations detected in strain Ab825 may have had a relevant impact on its pathogenic potential. These findings point to an impressive ability of *Aba* to quickly modify its genome in order to evade both natural host defenses and antibiotic intervention.

Author contributions
G.R., S.P.S., A.S.L and A.M.V. conceived and designed the work. M.M.C., J.P. and G.R. conducted the bioinformatics and experimental analysis. All authors analysed the data and wrote the manuscript. All authors read and approved the final manuscript.

Conflicts of interest
The authors declare that the research was conducted in the absence of any commercial or financial relationships that could be construed as a potential conflict of interest.

Data Bibliography
A. baumannii Ab242 Repizo,G.D., Cameranesi,M., Limanksy,A.S., Moran Barrio,J. and Viale,A.M. NCBI NXGW00000000 (2017)

A. baumannii Ab244 Repizo,G.D., Cameranesi,M., Limanksy,A.S., Moran Barrio,J. and Viale,A.M. NCBI PGTR00000000 (2017)

A. baumannii Ab825 Repizo,G.D., Cameranesi,M. and Borges,V. NCBI NTFR00000000 (2017)

A. baumannii Ab244 pAb244-7 Cameranesi,M. Accession number MG520098 (2018)

References
1. Peleg AY, Seifert H, Paterson DL. *Acinetobacter baumannii*: emergence of a successful pathogen. *Clin Microbiol Rev* 2008;21:538–.
2. Antunes LCS, Visca P, Towner KJ. *Acinetobacter baumannii*: evolution of a global pathogen. *Pathog Dis* 2014;71:292–301.
3. Wong D, Nielsen TB, Bonomo RA, Pantapalangkoor P, Luna B *et al*. Clinical and pathophysiological overview of *Acinetobacter* infections: a century of challenges. *Clin Microbiol Rev* 2017;30:409–447.
4. Diancourt L, Passet V, Nemec A, Dijkshoorn L, Brisse S. The population structure of *Acinetobacter baumannii*: expanding multiresistant clones from an ancestral susceptible genetic pool. *PLoS One* 2010;5:e10034.
5. Roca I, Espinal P, Vila-Farrés X, Vila J. The *Acinetobacter baumannii* oxymoron: commensal hospital dweller turned pan-drug-resistant menace. *Front Microbiol* 2012;3:148.
6. Mussi M, Limansky A, Viale A. Acquisition of resistance to carbapenems in multidrug-resistant clinical strains of. *Antimicrobial Agents and Chemother* 2005;49:1432–1440.
7. Mussi MA, Relling VM, Limansky AS, Viale AM. CarO, an *Acinetobacter baumannii* outer membrane protein involved in

8. Mussi MA, Limansky AS, Relling V, Ravasi P, Arakaki A *et al*. Horizontal gene transfer and assortative recombination within the *Acinetobacter baumannii* clinical population provide genetic diversity at the single carO gene, encoding a major outer membrane protein channel. *J Bacteriol* 2011;193:4736–4748.
9. Ravasi P, Limansky AS, Rodriguez RE, Viale AM, Mussi MA. ISAba825, a functional insertion sequence modulating genomic plasticity and bla(OXA-58) expression in *Acinetobacter baumannii*. *Antimicrob Agents Chemother* 2011;55:917–920.
10. Morán-Barrio J, Cameranesi MM, Relling V, Limansky AS, Brambilla L *et al*. The *Acinetobacter* outer membrane contains multiple specific channels for carbapenem β-lactams as revealed by kinetic characterization analyses of imipenem permeation into *Acinetobacter* baylyi cells. *Antimicrob Agents Chemother* 2017;61
11. Tacconelli E, Carrara E, Savoldi A, Harbarth S, Mendelson M *et al*. Discovery, research, and development of new antibiotics: the who priority list of antibiotic-resistant bacteria and tuberculosis. *Lancet Infect Dis* 2018;18:318–.
12. Touchon M, Cury J, Yoon E-J, Krizova L, Cerqueira GC *et al*. The genomic diversification of the whole *Acinetobacter* genus: origins, mechanisms, and consequences. *Genome Biol Evol* 2014;6:2866–2882.
13. Harding CM, Hennon SW, Feldman MF. Uncovering the mechanisms of *Acinetobacter baumannii* virulence. *Nat Rev Microbiol* 2018;16:91–102.
14. Lee C-R, Lee JH, Park M, Park KS, Bae IK *et al*. Biology of *Acinetobacter baumannii*: Pathogenesis, Antibiotic Resistance Mechanisms, and Prospective Treatment Options. *Front Cell Infect Microbiol* 2017;7:55.
15. Nigro SJ, Post V, Hall RM. The multiresistant *Acinetobacter baumannii* European clone I type strain RUH875 (A297) carries a genomic antibiotic resistance island AbaR21, plasmid pRAY and a cluster containing ISAba1-sul2-CR2-strB-strA. *J Antimicrob Chemother* 2011;66:1928–1930.
16. Chan AP, Sutton G, DePew J, Krishnakumar R, Choi Y *et al*. A novel method of consensus pan-chromosome assembly and large-scale comparative analysis reveal the highly flexible pan-genome of *Acinetobacter baumannii*. *Genome Biol* 2015;16:143.
17. Nigro SJ, Hall RM. Structure and context of *Acinetobacter* transposons carrying the oxa23 carbapenemase gene. *J Antimicrob Chemother* 2016;71:1135–1147.
18. Blackwell GA, Hall RM. The tet39 Determinant and the msrE-mphE Genes in *Acinetobacter* Plasmids Are Each Part of Discrete Modules Flanked by Inversely Oriented pdif (XerC-XerD) Sites. *Antimicrob Agents Chemother* 2017;61
19. Adams MD, Bishop B, Wright MS. Quantitative assessment of insertion sequence impact on bacterial genome architecture. *Microb Genom* 2016;2:e000062.
20. Wright MS, Mountain S, Beeri K, Adams MD. Assessment of insertion sequence mobilization as an adaptive response to oxidative stress in *Acinetobacter baumannii* using IS-seq. *J Bacteriol* 2017;199
21. Karah N, Sundsfjord A, Towner K, Samuelsen Ørjan. Insights into the global molecular epidemiology of carbapenem non-susceptible clones of *Acinetobacter baumannii*. *Drug Resist Updat* 2012;15:237–247.
22. Geisinger E, Huo W, Hernandez-Bird J, Isberg RR. *Acinetobacter baumannii*: Envelope Determinants That Control Drug Resistance, Virulence, and Surface VariEnvelope Determinants That Control Drug Resistance, Virulence, and Surface Variability. *Annu Rev Microbiol* 2019;73:481–506.
23. Repizo GD, Viale AM, Borges V, Cameranesi MM, Taib N *et al*. The environmental *Acinetobacter baumannii* isolate DSM30011 reveals clues into the preantibiotic era genome diversity, virulence potential, and niche range of a predominant nosocomial pathogen. *Genome Biol Evol* 2017;9:2292–.

24. Yakkala H, Samantarrai D, Gribskov M, Siddavattam D. Comparative genome analysis reveals niche-specific genome expansion in *Acinetobacter baumannii* strains. *PLoS One* 2019;14:e0218204.

25. Snitkin ES, Zelazny AM, Montero CI, Stock F, Mijares L *et al*. Genome-Wide recombination drives diversification of epidemic strains of *Acinetobacter baumannii*. *Proc Natl Acad Sci U S A* 2011;108:13758–13763.

26. Wright MS, Haft DH, Harkins DM, Perez F, Hujer KM *et al*. New insights into dissemination and variation of the health care-associated pathogen *Acinetobacter baumannii* from genomic analysis. *mBio* 2014;5:e00963-13.

27. Limansky AS, Zamboni MI, Guardati MC, Rossignol G, Campos E *et al*. Evaluation of phenotypic and genotypic markers for clinical strains of *Acinetobacter baumannii*. *Medicina* 2004;64:306–312.

28. Mussi MA, Limansky AS, Viale AM. Acquisition of resistance to carbapenems in multidrug-resistant clinical strains of *Acinetobacter baumannii*: natural insertional inactivation of a gene encoding a member of a novel family of beta-barrel outer membrane proteins. *Antimicrob Agents Chemother* 2005;49:1432–1440.

29. Clinical and Laboratory Standards Institute. *Performance Standards for Antimicrobial Susceptibility Testing, Document M100S*, 26th ed. Wayne, PA; 2016.

30. Darling AE, Mau B, Perna NT. ProgressiveMauve: multiple genome alignment with gene gain, loss and rearrangement. *PLoS One* 2010;5:e11147.

31. Gao F, Zhang C-T. Ori-Finder: a web-based system for finding oriCs in unannotated bacterial genomes. *BMC Bioinformatics* 2008;9:79.

32. Siguier P, Perochon J, Lestrade L, Mahillon J, Chandler M. ISfinder: the reference centre for bacterial insertion sequences. *Nucleic Acids Res* 2006;34:D32–.

33. Arndt D, Grant JR, Marcu A, Sajed T, Pon A *et al*. PHASTER: a better, faster version of the PHAST phage search tool. *Nucleic Acids Res* 2016;44:W16–.

34. Zankari E, Hasman H, Cosentino S, Vestergaard M, Rasmussen S *et al*. Identification of acquired antimicrobial resistance genes. *J Antimicrob Chemother* 2012;67:2640–2644.

35. Jolley KA, Maiden MCJ. BIGSdb: scalable analysis of bacterial genome variation at the population level. *BMC Bioinformatics* 2010;11:595.

36. Antunes LCS, Imperi F, Towner KJ, Visca P. Genome-Assisted identification of putative iron-utilization genes in *Acinetobacter baumannii* and their distribution among a genotypically diverse collection of clinical isolates. *Res Microbiol* 2011;162:279–.

37. Repizo GD, Gagné S, Foucault-Grunenwald M-L, Borges V, Charpentier X *et al*. Differential role of the T6SS in *Acinetobacter baumannii* virulence. *PLoS One* 2015;10:e0138265.

38. Clímaco EC, Oliveira MLde, Pitondo-Silva A, Oliveira MG, Medeiros M *et al*. Clonal complexes 104, 109 and 113 playing a major role in the dissemination of OXA-carbapenemase-producing *Acinetobacter baumannii* in Southeast Brazil. *Infect Genet Evol* 2013;19:127–133.

39. Stietz MS, Ramírez MS, Vilacoba E, Merkier AK, Limansky AS *et al*. *Acinetobacter baumannii* extensively drug resistant lineages in Buenos Aires hospitals differ from the International clones I-III. *Infect Genet Evol* 2013;14:294–301.

40. Smith MG, Gianoulis TA, Pukatzki S, Mekalanos JJ, Ornston LN *et al*. New insights into *Acinetobacter baumannii* pathogenesis revealed by high-density pyrosequencing and transposon mutagenesis. *Genes Dev* 2007;21:601–614.

41. Repizo GD, Esparz M, Seravalle JL, Salcedo SP. Bioinformatic analysis of the type VI secretion system and its potential toxins in the *Acinetobacter* genus. *Front Microbiol* 2019;10.

42. De Gregorio E, Zarrilli R, Di Nocera PP. Contact-dependent growth inhibition systems in *Acinetobacter*. *Sci Rep* 2019;9:154.

43. Roussin M, Rabarioelina S, Cluzeau L, Cayron J, Lesterlin C *et al*. Identification of a Contact-Dependent Growth Inhibition (CDI) System That Reduces Biofilm Formation and Host Cell Adhesion of *Acinetobacter baumannii* DSM30011 Strain. *Front Microbiol* 2019;10:2450.

44. Wright MS, Haft DH, Harkins DM, Perez F, Hujer KM *et al*. New insights into dissemination and variation of the health care-associated pathogen *Acinetobacter baumannii* from genomic analysis. *mBio* 2014;5:e00963-13.

45. Kim DH, Jung S-I, Kwon KT, Ko KS. Occurrence of diverse AbGRI1-type genomic islands in *Acinetobacter baumannii* global clone 2 isolates from South Korea. *Antimicrob Agents Chemother* 2017;61

46. Seputiene V, Povilonis J, Sužiedeliene E. Novel variants of AbaR resistance islands with a common backbone in *Acinetobacter baumannii* isolates of European clone II. *Antimicrob Agents Chemother* 2012;56:1969–1973.

47. Post V, White PA, Hall RM. Evolution of AbaR-type genomic resistance islands in multiply antibiotic-resistant *Acinetobacter baumannii*. *J Antimicrob Chemother* 2010;65:1162–1170.

48. Liu F, Zhu Y, Yi Y, Lu N, Zhu B *et al*. Comparative genomic analysis of *Acinetobacter baumannii* clinical isolates reveals extensive genomic variation and diverse antibiotic resistance determinants. *BMC Genomics* 2014;15:1163.

49. Al-Jabri Z, Zamudio R, Horvath-Papp E, Ralph JD, Al-Muharrami Z *et al*. Integrase-Controlled Excision of Metal-Resistance Genomic Islands in *Acinetobacter baumannii*. *Genes* 2018;9:366

50. Farrugia DN, Elbourne LDH, Mabbutt BC, Paulsen IT. A novel family of integrases associated with prophages and genomic islands integrated within the tRNA-dihydrouridine synthase A (*dusA*) gene. *Nucleic Acids Res* 2015;43:4547–4557.

51. Ghisotti D, Finkel S, Halling C, Dehò G, Sironi G *et al*. Nonessential region of bacteriophage P4: DNA sequence, transcription, gene products, and functions. *J Virol* 1990;64:24–36.

52. Costa AR, Monteiro R, Azeredo J. Genomic analysis of *Acinetobacter baumannii* prophages reveals remarkable diversity and suggests profound impact on bacterial virulence and fitness. *Sci Rep* 2018;8:15346.

53. Babu MM, Iyer LM, Balaji S, Aravind L. The natural history of the WRKY-GCM1 zinc fingers and the relationship between transcription factors and transposons. *Nucleic Acids Res* 2006;34:6505–.

54. Eaves-Pyles T, Allen CA, Taormina J, Swidsinski A, Tutt CB *et al*. Escherichia coli isolated from a Crohn's disease patient adheres, invades, and induces inflammatory responses in polarized intestinal epithelial cells. *Int J Med Microbiol* 2008;298:397–409.

55. Chai B, Wang H, Chen X. Draft genome sequence of high-melanin-yielding Aeromonas media strain Ws. *J Bacteriol* 2012;194:6693–.

56. Carattoli A. Plasmids and the spread of resistance. *Int J Med Microbiol* 2013;303:298–304.

57. Cameranesi MM, Morán-Barrio J, Limansky AS, Repizo GD, Viale AM. Site-Specific Recombination at XerC/D Sites Mediates the Formation and Resolution of Plasmid Co-integrates Carrying a *bla*$_{OXA-58}$- and Tn*aphA6*-Resistance Module in *Acinetobacter baumannii*. *Front Microbiol* 2018;9:66.

58. Mindlin S, Beletsky A, Mardanov A, Petrova M. Adaptive dif modules in permafrost strains of *Acinetobacter lwoffii* and their distribution and abundance among present day *Acinetobacter* strains. *Front Microbiol* 2019;10:1–11.

59. Brovedan M, Repizo GD, Marchiaro P, Viale AM, Limansky A. Characterization of the diverse plasmid pool harbored by the blaNDM-1-containing *Acinetobacter bereziniae* HPC229 clinical strain. *PLoS One* 2019;14:e0220584.

60. Evans BA, Amyes SGB. Oxa β-lactamases. *Clin Microbiol Rev* 2014;27:241–263.

61. Lopes BS, Amyes SGB. Role of ISAba1 and ISAba125 in governing the expression of blaADC in clinically relevant *Acinetobacter baumannii* strains resistant to cephalosporins. *J Med Microbiol* 2012;61:1103–.

62. Segal H, Jacobson RK, Garny S, Bamford CM, Elisha BG. Extended -10 promoter in ISAba-1 upstream of blaOXA-23 from *Acinetobacter baumannii. Antimicrob Agents Chemother* 2007;51:3040–3041.

63. Tian G-B, Adams-Haduch JM, Taracila M, Bonomo RA, Wang H-N *et al*. Extended-Spectrum AmpC cephalosporinase in *Acinetobacter baumannii*: ADC-56 confers resistance to cefepime. *Antimicrob Agents Chemother* 2011;55:4922–4925.

64. Perreten V, Boerlin P. A new sulfonamide resistance gene (sul3) in Escherichia coli is widespread in the pig population of Switzerland. *Antimicrob Agents Chemother* 2003;47:1169–1172.

65. Byrne-Bailey KG, Gaze WH, Kay P, Boxall ABA, Hawkey PM *et al*. Prevalence of sulfonamide resistance genes in bacterial isolates from manured agricultural soils and pig slurry in the United Kingdom. *Antimicrob Agents Chemother* 2009;53:696–702.

66. Post V, White PA, Hall RM. Evolution of AbaR-type genomic resistance islands in multiply antibiotic-resistant *Acinetobacter baumannii. J Antimicrob Chemother* 2010;65:1162–1170.

67. Hamidian M, Hall RM. The resistance gene complement of D4, a multiply antibiotic-resistant ST25 *Acinetobacter baumannii* isolate, resides in two genomic islands and a plasmid. *J Antimicrob Chemother* 2016;71:1730–1732.

68. Falagas ME, Vardakas KZ, Roussos NS. Trimethoprim/Sulfamethoxazole for *Acinetobacter* spp.: a review of current microbiological and clinical evidence. *Int J Antimicrob Agents* 2015;46:231–241.

69. Lawley TD, Burland V, Taylor DE. Analysis of the complete nucleotide sequence of the tetracycline-resistance transposon Tn10. *Plasmid* 2000;43:235–239.

70. Peleg AY, Jara S, Monga D, Eliopoulos GM, Moellering RC *et al*. Galleria mellonella as a model system to study *Acinetobacter baumannii* pathogenesis and therapeutics. *Antimicrob Agents Chemother* 2009;53:2605–2609.

71. Lee C-R, Lee JH, Park M, Park KS, Bae IK *et al*. Biology of *Acinetobacter baumannii*: Pathogenesis, Antibiotic Resistance Mechanisms, and Prospective Treatment Options. *Front Cell Infect Microbiol* 2017;7:55.

72. Iwashkiw JA, Seper A, Weber BS, Scott NE, Vinogradov E *et al*. Identification of a general O-linked protein glycosylation system in *Acinetobacter baumannii* and its role in virulence and biofilm formation. *PLoS Pathog* 2012;8:e1002758.

73. Kenyon JJ, Hall RM. Variation in the complex carbohydrate biosynthesis loci of *Acinetobacter baumannii* genomes. *PLoS One* 2013;8:e62160.

74. Singh JK, Adams FG, Brown MH. Diversity and function of capsular polysaccharide in *Acinetobacter baumannii*.*Front Microbiol* 2019;10:1–8.

75. Hu D, Liu B, Dijkshoorn L, Wang L, Reeves PR. Diversity in the major polysaccharide antigen of *Acinetobacter baumannii* assessed by DNA sequencing, and development of a molecular serotyping scheme. *PLoS One* 2013;8:e70329–13.

76. Liu MA, Morris P, Reeves PR. Wzx flippases exhibiting complex O-unit preferences require a new model for Wzx-substrate interactions. *Microbiologyopen* 2019;8:e00655.

77. Kenyon JJ, Nigro SJ, Hall RM. Variation in the OC locus of *Acinetobacter baumannii* genomes predicts extensive structural diversity in the lipooligosaccharide. *PLoS One* 2014;9:e107833.

78. Gaddy JA, Arivett BA, McConnell MJ, López-Rojas R, Pachón J *et al*. Role of acinetobactin-mediated iron acquisition functions in the interaction of *Acinetobacter baumannii* strain ATCC 19606T with human lung epithelial cells, Galleria mellonella caterpillars, and mice. *Infect Immun* 2012;80:1015–1024.

79. Mortensen BL, Skaar EP. The contribution of nutrient metal acquisition and metabolism to *Acinetobacter baumannii* survival within the host. *Front Cell Infect Microbiol* 2013;3:95.

80. Runci F, Gentile V, Frangipani E, Rampioni G, Leoni L *et al*. Contribution of active iron uptake to *Acinetobacter baumannii* pathogenicity. *Infect Immun* 2019;87

81. Gaddy JA, Arivett BA, McConnell MJ, López-Rojas R, Pachón J, Actis LA, Rafael LR *et al*. Role of acinetobactin-mediated iron acquisition functions in the interaction of *Acinetobacter baumannii* strain ATCC 19606T with human lung epithelial cells, *Galleria mellonella caterpillars*, and mice. *Infect Immun* 2012;80:1015–1024.

82. Ou H-Y, Kuang SN, He X, Molgora BM, Ewing PJ *et al*. Complete genome sequence of hypervirulent and outbreak-associated *Acinetobacter baumannii* strain LAC-4: epidemiology, resistance genetic determinants and potential virulence factors. *Sci Rep* 2015;5:8643.

83. Penwell WF, DeGrace N, Tentarelli S, Gauthier L, Gilbert CM *et al*. Discovery and characterization of new hydroxamate siderophores, Baumannoferrin A and B, produced by *Acinetobacter baumannii. Chembiochem* 2015;16:1896–1904.

84. Waack U, Warnock M, Yee A, Huttinger Z, Smith S *et al*. CpaA is a glycan-specific Adamalysin-like protease secreted by *Acinetobacter baumannii* that inactivates coagulation factor XII. *mBio* 2018;9:e01606-18

85. Weber BS, Harding CM, Feldman MF. Pathogenic *Acinetobacter*: from the cell surface to infinity and beyond. *J Bacteriol* 2016;198:880–887.

86. Harding CM, Pulido MR, Di Venanzio G, Kinsella RL, Webb AI *et al*. Pathogenic *Acinetobacter* species have a functional type I secretion system and contact-dependent inhibition systems. *J Biol Chem* 2017;292:9075–9087.

87. Pierson LS, Pierson EA. Metabolism and function of phenazines in bacteria: impacts on the behavior of bacteria in the environment and biotechnological processes. *Appl Microbiol Biotechnol* 2010;86:1659–.

88. Karuppiah V, Thistlethwaite A, Dajani R, Warwicker J, Derrick JP. Structure and mechanism of the bifunctional CinA enzyme from *Thermus thermophilus. J Biol Chem* 2014;289:33187–33197.

89. Eijkelkamp BA, Stroeher UH, Hassan KA, Paulsen IT, Brown MH. Comparative analysis of surface-exposed virulence factors of *Acinetobacter baumannii. BMC Genomics* 2014;15:1020.

90. Zeidler S, Müller V. Coping with low water activities and osmotic stress in *Acinetobacter baumannii*: significance, current status and perspectives. *Environ Microbiol* 2019;21:2212–2230.

91. Stahl J, Bergmann H, Göttig S, Ebersberger I, Averhoff B. *Acinetobacter baumannii* virulence is mediated by the concerted action of three phospholipases D. *PLoS One* 2015;10:e0138360–19.

92. Weber BS, Hennon SW, Wright MS, Scott NE, de Berardinis V *et al*. Genetic dissection of the type VI secretion system in *Acinetobacter* and identification of a novel peptidoglycan hydrolase, TagX, required for its biogenesis. *mBio* 2016;7:e01253-16

93. Li L, Wang Y-N, Jia H-B, Wang P, Dong J-F *et al*. The type VI secretion system protein AsaA in *Acinetobacter baumannii* is a periplasmic protein physically interacting with TssM and required for T6SS assembly. *Sci Rep* 2019;9:9438.

94. Jones CL, Clancy M, Honnold C, Singh S, Snesrud E *et al*. Fatal outbreak of an emerging clone of extensively drug-resistant *Acinetobacter baumannii* with enhanced virulence. *Clin Infect Dis* 2015;61:145–154.

95. Repizo GD. Prevalence of *Acinetobacter baumannii* strains expressing the type 6 secretion system in patients with bacteremia. *Virulence* 2017;8:1099–.

96. Gebhardt MJ, Gallagher LA, Jacobson RK, Usacheva EA, Peterson LR *et al*. Joint transcriptional control of virulence and resistance to antibiotic and environmental stress in *Acinetobacter baumannii. mBio* 2015;6:e01660-15.

97. Di Venanzio G, Moon KH, Weber BS, Lopez J, Ly PM *et al*. Multidrug-resistant plasmids repress chromosomally encoded T6SS to enable their dissemination. *Proc Natl Acad Sci U S A* 2019;116:1378–1383.

98. Zhang L, Liang W, Shu-Gen Xu JM, Di Y-Y LH-H, Wang Y *et al*. CarO promotes adhesion and colonization of *Acinetobacter baumannii* through inhibiting NF-κB pathways. *Int J Clin Exp Med* 2019;12:2518–2524.

99. Clímaco EC, Oliveira MLde, Pitondo-Silva A, Oliveira MG, Medeiros M *et al.* Clonal complexes 104, 109 and 113 playing a major role in the dissemination of OXA-carbapenemase-producing *Acinetobacter baumannii* in Southeast Brazil. *Infect Genet Evol* 2013;19:127–133.

100. Ramírez MS, Vilacoba E, Stietz MS, Merkier AK, Jeric P *et al.* Spreading of AbaR-type genomic islands in multidrug resistance *Acinetobacter baumannii* strains belonging to different clonal complexes. *Curr Microbiol* 2013;67:9–14.

101. Palmer KL, Gilmore MS. Multidrug-Resistant enterococci lack CRISPR-Cas. *mBio* 2010;1:e00227-10